Hydrogen assisted cracking in a high strength dual phase steel DP1180HY

Benjamin Kröger, Reinhold Holbein, Friedrichshafen, and Stephan G. Klose, Sindelfingen, Germany

Article Information

Correspondence Address
Benjamin Kröger, M.Sc.
Steinbeis-Transferzentrum
Werkstoffe Korrosion und Korrosionsschutz GmbH
Hermann-Metzger-Str. 5
D-88045 Friedrichshafen, Germany
E-mail: kroeger@stz-werkstoffe.de

Keywords
UHSS steel, delayed fracture, diffusible hydrogen, cathodic-type hydrogen charging, hydrogen embrittlement, four-point-bending, U-bend

Important objectives when using high strength steel materials in the automotive industry are to reduce the weight and therefore the energy consumption of motor vehicles. Suitable test methods must be used to characterize the material specific properties in relation to hydrogen induced effects so that the materials can be used safely in body structures. Strained bend specimens and 4-point loaded specimens were used for this work. Both test methods have specific advantages and disadvantages and provide meaningful results in regard to the time delay in hydrogen assisted brittle fractures. Fundamental insights were obtained regarding the test procedure and the development of test methods for the impact of hydrogen on steel during manufacture and operation of respective components.

Important objectives when using materials in the automotive industry are to reduce the weight and therefore the energy consumption of motor vehicles. It is known that the sensitivity of high strength steels to hydrogen degradation increases with increasing strength. The sources of hydrogen can be either the manufacturing conditions and/or the operational conditions. Depending on the type of source of hydrogen, diffusive and nondiffusive hydrogen concentrations can lead to hydrogen assisted cracking. It is essential to know the sensitivity of high strength steel sheet materials to hydrogen in order to use them safely. Hydrogen assisted stress-corrosion cracking is known to be triggered by a medium in conjunction with a mechanical load above a threshold value (critical tensile strain) [1, 2].

According to Pöpperling [1], the critical tensile stress can be below 10 % of the yield strength in high strength steels with a tensile strength > 900 MPa depending on the hydrogen activity. The concentration of diffusive and nondiffusive hydrogen which leads to hydrogen induced damage is also dependent on the microstructural properties of the material in a real component. Hydrogen can lead to fatal break of structural parts due to hydrogen assisted cracking depending on hydrogen concentration and mechanical stress. Furthermore, the ductility and forming limits are reduced owing to the presence of hydrogen by degradation of the material [3]. According to Loidl [4], even minimal hydrogen concentrations have an influence on the ductility of high strength dual phase steel. Qualitative determining factors are shown schematically in the Figures 1a and 1b.

Hydrogen charging procedure in relation to various test methods

Various test methods are used for a quantitative determination of the determining factors. Critical mechanical stresses for hydrogen assisted cracking can be determined via tests such as slow strain rate tests or a step load test. Using these tests, the critical mechanical stress (onset of cracking) is deter-

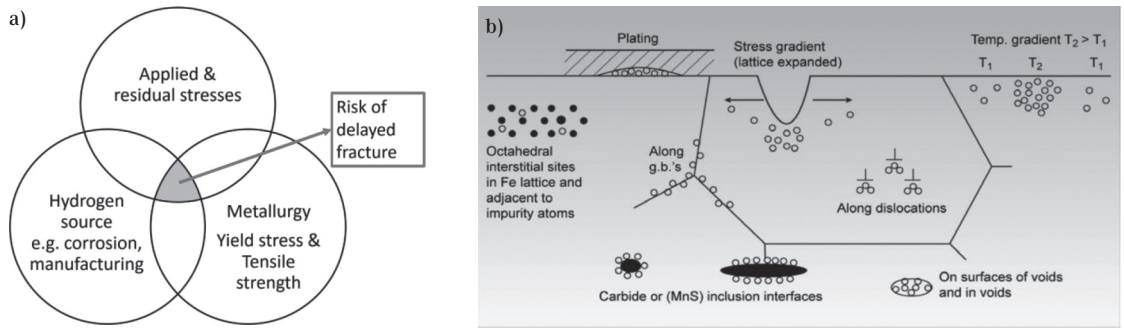

Figure 1: Determining factors, a) general factors, b) material dependent effects, according to Vanhill et al. [5]

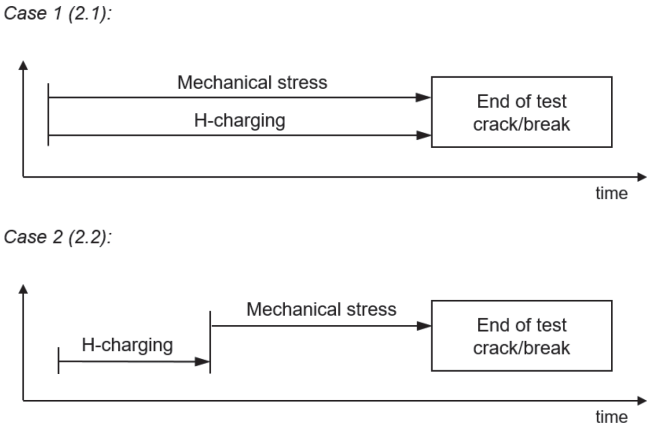

Figure 2: Sequence of hydrogen charging and mechanical testing

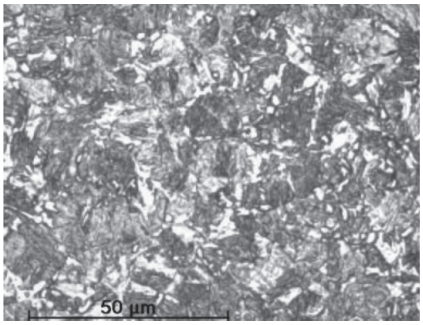

Figure 3: Dual phase steel DP1180HY, micrograph etched with 3 % alcoholic HNO_3 (martensite (dark), ferrite (light)) [6]

mined by varying the mechanical stress under constant hydrogen charging.

Component related test methods must be used to quantify component related factors such as the shape or shear cutting.

At the same time, it is also necessary to determine at which time the hydrogen penetrates the material. Where the penetration of hydrogen is due to corrosion attack, for example, the component is already under mechanical stress during hydrogen penetration (see Case 1, Figure 2). With hydrogen diffusion, which is due to production, such as electroplating, the hydrogen enters the component before it is subjected to mechanical stress (see Case 2, Figure 2).

The aim of this work is to investigate the behavior of a steel sample charged with hydrogen under electrochemical controlled conditions in relation to the hydrogen assisted damage of diffusible hydrogen. This is done under four different conditions with a bend specimen geometry and a 4-point loaded specimen geometry. In this case, the specimen is charged with hydrogen once under mechanical load and once without mechanical loading, as shown in Figure 2.

The hydrogen assisted fracture behavior results should be examined in correlation with the diffusible hydrogen concentration of the specimens.

The two test methods are compared with each other based on all the results and the suitability is determined in terms of delayed cracking due to hydrogen.

Material

The investigations are carried out using the commercially available steel material DP1180HY. This dual phase steel has a ferritic microstructure with embedded martensitic phases. The mechanical properties are listed in Table 1.

Figure 3 shows the distribution of martensite and ferrite in a metallographic micrograph [6]. The specimens are analyzed in the noncoated and nonprestretched state from the coil as supplied.

Description of test procedures

The specimens were prepared by shearing them from commercially available strip material with thickness t = 1.05 mm.

Bend specimens. The specimens are bent using a manual bending fixture. From our experience, the author found it necessary to provide a precise description of the bending process to obtain reproducible results. The specimen geometry is shown in Figure 4 and the folding process in Figure 5. The mandrel radius is r = 10 mm. After bending the specimen, the mechanical tension is maintained by holding it with a nut and bolt. The mechanical stress always lies above the yield strength in the plastic range. According to Equation (1), the near surface elongation of the outer bending radius is 5.76 % at t = 1.05 mm and r = 10 mm.

$$\varepsilon_{eq} = \frac{t}{(2R+t)}\frac{2}{\sqrt{3}} \qquad (1)$$

The intrinsic stresses introduced by shearing and plastic deformation at the edge are not recorded by this information. This must be taken into consideration when discussing the results later on.

The specimens are masked by applying an electrically insulating coating to an area of

Table 1: Mechanical properties of DP1180HY [6]

Direction	Yield strength (MPa)	Tensile strength (MPa)
Rolling	980	1191
Transverse	1037	1205

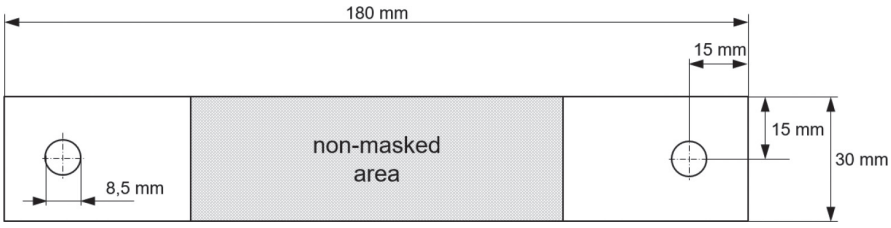

Figure 4: Geometry of the plane bend specimen

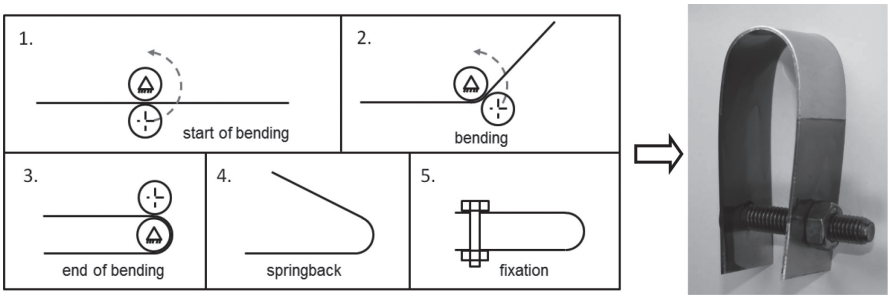

Figure 5: Schematic representation of the folding process for preparing the bend specimens and exemplary bent specimen

30 × 60 mm². The specimen is charged with hydrogen on the nonmasked area at the outer bending radius on the area of maximum strain.

4-point loaded specimens. The specimen geometry is shown in Figure 6. The 4-point loaded specimens are clamped in a load frame according to ASTM G39-1999 in Figure 7. The mechanical load (bending stress) of the specimen is calculated according to ASTM G39-1999 by Equation (2) [7]:

$$\sigma = \frac{12Ety}{(3H^2 - 4A^2)} \quad (2)$$

with: σ: maximum tensile stress, E: modulus of elasticity, t: sheet thickness (mm), y: maximum sheet deflection between the outer supports, H: distance between the outer supports in relation to the central axis and A: distance between the inner and outer supports in relation to the central axis.

The following stress boundary conditions are set in order to record both the elastic and the plastic range (yield strength 980 MPa):

- Elastic range: s = 700, 800 and 900 MPa
- Transition from elastic-plastic range: s = 1000 and 1100 MPa

The intrinsic stresses introduced by shearing and plastic deformation at the edge are not recorded by this information. This must be taken into consideration when discussing the results later on.

The specimens are masked by applying an electrically insulating coating up to an area of 30 × 60 mm² at the outer bending radius on the area of maximum strain for charging with hydrogen.

Test and hydrogen charging procedure for bend specimens and 4-point loaded specimens. In both Cases 1 and 2, the specimens were charged with hydrogen at a current density of 3.03 mA × cm⁻² in 3 wt.-% sodium chloride aqueous solution containing 0.3 wt-% KSCN as a promoter at a pH value of 5.8 to 5.9. Platinized titanium is used as counter electrode (CE). The test setup is shown in Figure 7. The load frames for the 4-point bending tests are made of polyoxymethylene. This material was chosen because of its good machinability, high dimensional stability and rigidity.

The following procedure is carried out for all specimens:

1. Preliminary test
   Determination of the maximum duration of hydrogen charging in the electrolyte t_B is the time at which the specimen shows the onset of cracks ≤ 1 mm long (depending on the material, mechanical load and geometry).

2.1 Charging with hydrogen under mechanical stress
   - I. Charging with hydrogen at 70 % t_B under load
   - II Maintaining the mechanical stress for up to 200 hours (without additional hydrogen charging)

2.2 Charging with hydrogen without mechanical stress
   - I. Charging with hydrogen at 70 % t_B without load
   - II. Subsequent mechanical loading up to 200 hours (without additional hydrogen charging)

The top start value was randomly set at 70 % t_B. In the investigation, this start value is gradually reduced in the U-bend specimens in order to determine the minimum value at which delayed cracking still occurs.

Measurement of diffusible hydrogen concentration. An apparatus for TDA measurements was used to measure the diffusible hydrogen on selected specimens. The measurements were carried out by ArcelorMittal R&D. This method is a carrier gas method shown in Figure 8a, in which the sample is heated at a fixed heating rate and the H_2 concentration is measured in the N_2 gas using a quadrupole mass spectrometer (calibrated with 50 ppm H_2/N_2 gas). Figure 8b shows an example for measurement. In this case, the heating rate is low so that the different desorption peaks are well re-

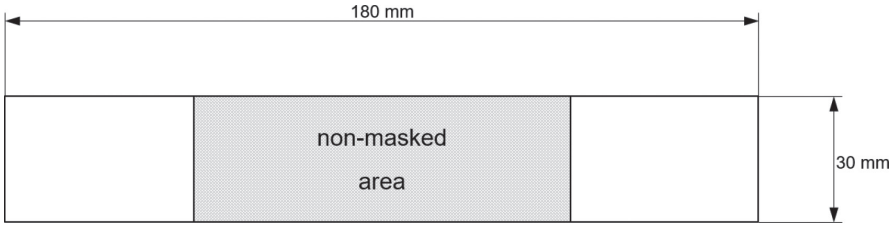

Figure 6 : 4-point loaded specimen and geometry of the sheet specimens

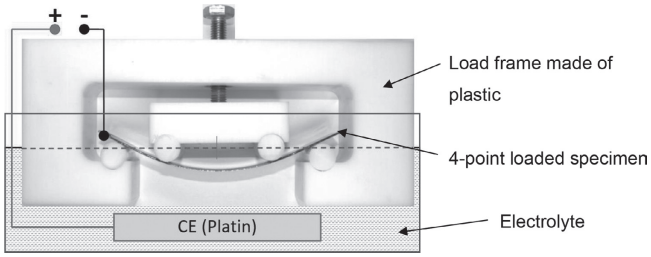

Figure 7: Test setup for 4-point bending test

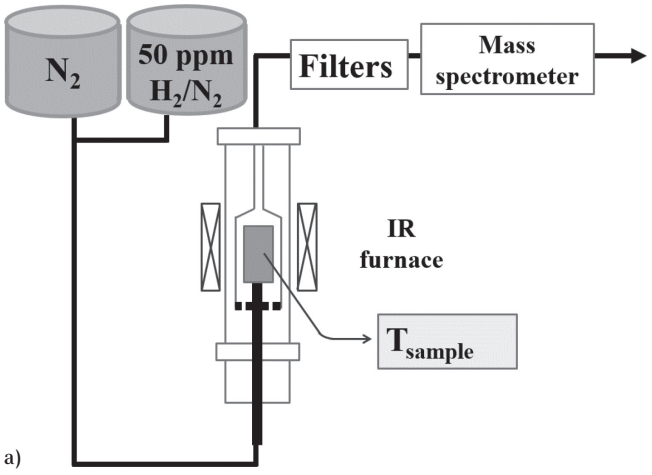

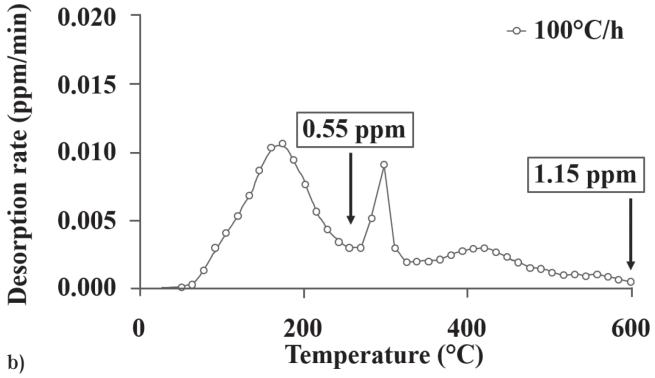

Figure 8: a) Synoptic of the TDA used at ArcelorMittal R&D [6], b) example of TDA signal obtained on precharged EG coated material [6]

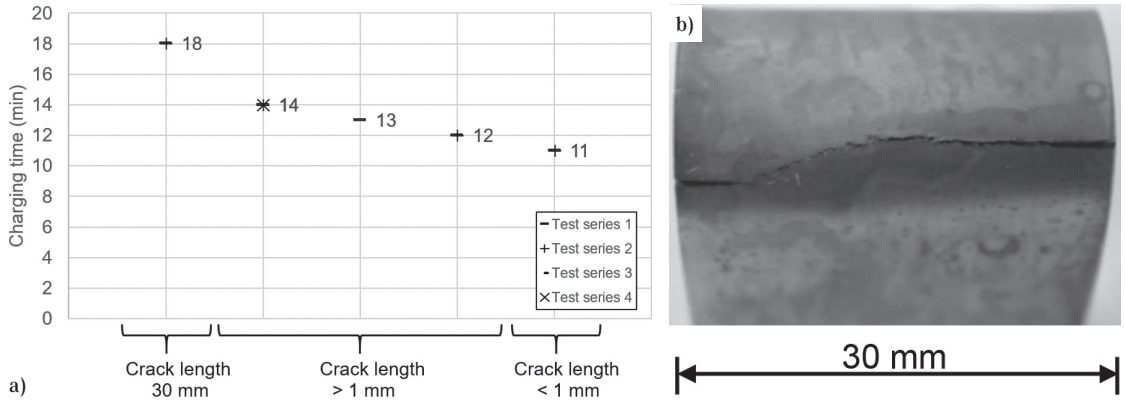

Figure 9: a) Preliminary tests, charging bend specimens with hydrogen for different durations and hydrogen assisted crack length, b) example of hydrogen assisted fracture on the bending radius, perpendicular to the maximum tensile stress of the U-bend specimen after a charging time of 18 minutes

solved (deconvolution). The first peak corresponds to the diffusible hydrogen (e. g., concentration of 0.55 ppm after integration up to 250 °C) [6]. The advantage of this device is that the measurement can be carried out on bare and coated material (e. g., Zn or e-coated). In this investigation, the diffusible hydrogen concentration was measured on bare material to prevent barrier effects by coatings, measurement was done by integration up to 250 °C.

The scatter of diffusive and nondiffusive hydrogen concentrations measured by TDA is affected by the apparatus used as well as other factors. A typical value for the standard deviation of specimens containing diffusive and nondiffusive hydrogen measured by a quadrupole mass spectrometer is 0.185 ppm for the diffusive hydrogen concentration [8]. The measured values are therefore discussed in relation to their unique tendencies and they are not absolute values.

Measurements on different coils showed that the hydrogen concentration is usually less than 0.1 ppm. The safety limit has been defined as 0.15 ppm in order to provide a wide safety margin [9].

Results

Preliminary tests to determine the charging time t_B with hydrogen. Preliminary tests of different duration were carried to determine the charging time t_B until the onset of hydrogen assisted cracking under load. In this case, the time was determined at which hydrogen assisted cracking was found to start with a crack length ≤ 1 mm. The onset of hydrogen assisted cracking was determined by light microscopy.

The crack always appears at the sheared edge on the outer radius, i. e., in the area of maximum tensile stress. The crack growth on the bend specimens and the 4-point loaded specimens runs at an angle of approx. 90° to the direction of maximum tensile stress. The crack length increases with charging time as shown in Figure 9a.

Results from preliminary U-bend tests. The initial charging time of 18 minutes to break was gradually reduced. The number of specimens is not always the same because the test was only repeated until sufficient reproducibility was achieved. The number of specimens ranges from 1 to 4.

Figure 9a shows the duration of charging with hydrogen and the associated crack lengths.

No hydrogen assisted crack formation was observed with charging times less than 11 minutes. The first hydrogen assisted cracks appear with a charging time of 11 minutes (t_B) (see Figure 9a). Increasing the charging time causes crack growth until the bend specimen fractures completely at 18 minutes (see Figure 9b).

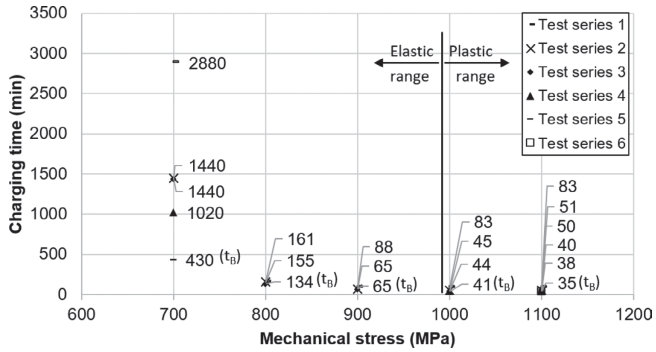

Figure 10: Preliminary test, load dependent hydrogen charging of different durations

Results from preliminary 4-point bend tests. Starting from 700 MPa, the load levels were increased in 100 MPa steps to 1100 MPa. The charging time for each load step was gradually reduced until the appearance of cracks < 1 mm (t_B). The number of specimens is not always the same because the test was only repeated until sufficient reproducibility was achieved. The number of specimens for each load level ranged between 3 and 6.

Figure 10 shows the charging time and load level for each specimen. The lowest point represents the time until the onset of cracking (t_B) based on a single measurement.

The charging time t_B until the onset of hydrogen assisted cracking depends on the mechanical stress. According to Figure 10, it is approx. 430 minutes in the elastic range at 700 MPa and 35 minutes in the plastic range at 1100 MPa.

Results from U-bend tests

Case 1 (charging under load). The upper start value was randomly set as the charging time 70 % of t_B (7 minutes 42 seconds). No hydrogen assisted cracks > 1 mm appeared after a charging time of 30 to 70 % of t_B. After charging has ended, hydrogen assisted cracking and crack growth occurred at different times (time delayed). The crack

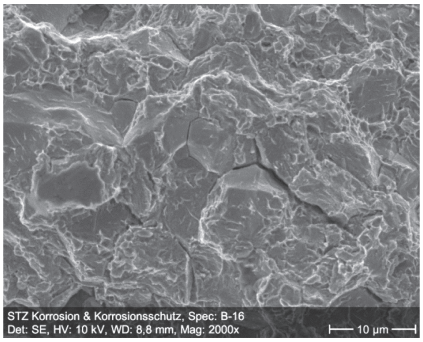

Figure 11: Scanning electron micrograph of the fracture surface of Specimen B-16

Specimen No.	Charging in % of t_B (min)	Hydrogen assisted crack length and duration of measurement					
		(h)	(mm)	(h)	(mm)	(h)	(mm)
B-13	70 % (7 min 42 s)	0	0.5	23	Fracture	–	–
B-14			0.5	24	Fracture	–	–
B-15	50 % (5 min 30 s)	0	0.0	48	7.00	200	8.10
B-16			0.0	24	Fracture	–	–
B-17	30 % (3 min 18 s)	0	0.0	48	6.30	200	7.50
B-18			0.0	48	8.40	200	9.70
B-19			0.7	16	Fracture	–	–
B-20			0.0	16	Fracture	–	–
B-21			0.0	24	8.57	200	13.31
B-22			0.0	24	0.78	200	1.12

Table 2: Results from U-bend specimens for charging under load and retention of load (Case 1)

Specimen No.	Charging in % of t_B (min)	Hydrogen assisted crack length and duration of measurement					
		(h)	(mm)	(h)	(mm)	(h)	(mm)
B-23	100 % (11 min)	0	0.0	64	10.22	200	10.22
B-24			0.0		Fracture		–
B-25			0.0		9.70		9.70
B-26			0.0		11.59		11.59
B-27			0.0		12.34		12.35
B-28			0.0		7.20		7.20
B-29			0.0		Fracture		–
B-30			0.0		Fracture		–
B-31			0.0		18.35		18.35
B-32			0.0		15.70		15.75

Table 3: Results from U-bend specimens for charging under no load and then application of load (Case 2)

Specimen No.	Bending stress σ (MPa)	Charging time 70 % t_B (min)	Hydrogen assisted crack length and duration of measurement					
			(h)	(mm)	(h)	(mm)	(h)	(mm)
4P-22	1100	24.5	0	0.0	24	0.00	200	0.00
4P-23				2.0		2.0		2.86
4P-24				0.0		0.67		0.67
4P-25				0.5		1.26		1.30
4P-26	1000	28.7	0	0.5	24	0.5	200	1.04
4P-27				0.0		0.0		1.81
4P-28				0.0		0.00		0.84
4P-29				0.0		0.00		0.00
4P-30	900	45.5	0	0.0	24	0.00	200	0.00
4P-31				0.0		0.00		0.00
4P-32				0.0		0.00		0.00
4P-33				0.0		0.00		0.00
4P-34	800	93.8	0	0.0	24	0.00	200	0.00
4P-35				0.0		0.00		0.00
4P-36				0.5		2.87		2.93
4P-37				0.0		0.00		0.00
4P-38	700	301	0	0.0	24	0.00	200	0.00

Table 4: Results from charging 4-point loaded specimens with hydrogen under load

always appears at the sheared edge. Scanning electron microscopic analysis of the fracture surface also shows residual ductile fractures as well as hydrogen assisted damage in the form of brittle fractures and gaping grain boundaries (see Figure 11).

Delayed hydrogen assisted cracking occurred for all charging times less than t_B. No dependency on the delay of charging time (amount of hydrogen) can be derived from these figures (see Table 2).

Case 2 (charging before the application of mechanical load). With a charging time of 100 % of t_B (11 minutes), delayed hydrogen assisted cracking or fractures occurred after the application of mechanical load. Three out of ten specimens were fractured within a test duration of 64 hours. The crack always appears at the sheared edge. Almost no crack growth and no further fractures were observed on the remaining specimens up to a test duration of 200 hours (see Table 3).

Results from 4-point loaded tests

Case 1 (Charging under mechanical load). The charging time of 70 % of t_B was randomly chosen as a start value. Delayed hydrogen assisted cracking occurs in the plastic range during the test in six out of eight specimens (1000 and 1100 MPa). Delayed hydrogen assisted cracking occurred in the elastic range (< 1000 MPa) after 24 hours in one out of eight specimens. Thus, the higher the load the sooner and more frequent the delayed hydrogen assisted cracking.

2 mm cracks appeared on a single specimen at 1100 MPa immediately after charging.

Delayed crack growth was observed with increasing test duration after charging in seven out of seventeen specimens. There were no fractures. On all specimens, the cracks start out from the punched edge.

It is assumed that no hydrogen assisted crack formation can be expected for a test load of 700 MPa or less by this test method. Thus, no further specimens (see Table 4) were tested.

Case 2 (charging before the application of mechanical load). No delayed hydrogen assisted cracking or fractures occurred in six out of the seven specimens with a charging time of 100 % t_B. Delayed hydrogen assisted cracking occurred after 70 hours on a specimen with a load of 1100 MPa. The crack has not grown. Since no cracks occurred below 1100 MPa, the number of specimens was limited. Thus, no further specimens were tested below 700 MPa (see Table 5).

Scanning electron microscopic analyses of the fracture surface of the specimen with a crack show evidence of hydrogen assisted damage in the form of brittle fractures and gaping grain boundaries.

Results from the TDA measurements

Case 1 (charging under load). TDA measurements were carried out on each bend specimen which was charged under load at 30, 50, 70 and 100 % t_B (Case 1), respectively. A diffusible hydrogen concentration of 0.35 ppm was found for a charging time of 50 % t_B and up to 0.67 ppm for a charging time of 100 % t_B.

Measurements on two bend specimens charged at 100 % t_B under no load (Case 2) show an average diffusible hydrogen concentration of 0.45 ppm. The two different measurements of 0.39 ppm and 0.52 ppm are probably within the range of scatter for the measurement method.

The diffusible hydrogen concentration appears to increase with increasing duration. The measured values for 30 % and 50 % t_B hardly differ at 0.35 ppm and 0.36 ppm and are also probably within the range of scatter for the measurement method (see Table 6).

Case 2 (charging before applying the mechanical load). TDA measurements were carried out on each 4-point loaded specimen which was charged at 70 % t_B (load dependent) at the different load levels of 1100, 900 and 700 MPa. Diffusible hydrogen concentrations from 0.46 ppm (1100 MPa) to 0.9 ppm (700 MPa) were found.

Measurements carried out on three 4-point loaded specimens under no load charged at 100 % t_B (t_B is load dependent) show diffusible hydrogen concentration from 0.56 ppm to 1.31 ppm (see Table 6). The diffusible hydrogen concentration appears to increase with increasing duration. The measured values suggest that the uptake of hydrogen increases with increasing mechanical load to an unspecified saturation limit. The saturation limit is known for other charging methods and is, in addition to the charging time, also dependent on factors such as the degree of the deformation [10]. In this case, the mechanical load increases by 400 MPa and approx. ten times the charging time is required to achieve double the amount of diffusible hydrogen concentration.

Discussion

Test procedures. The behavior of high strength sheet material DP1180HY was investigated in response to hydrogen assisted damage based on 4-point loaded tests and bend specimens. The time sequence for charging and the time of load application were taken into consideration.

The advantage of both test methods is that they are easy to carry out and require little test equipment. Preparing both specimen types by cutting them out is very cheap and they can be produced in large quantities. The plastic deformation in the bending radius of the bend specimen means that it is suitable for investigating component-like conditions. The 4-point loaded specimen is suitable for basic investigations such as determining stress limits for hydrogen assisted damage. Table 7 shows a qualitative evaluation.

In the first step, for two specimen types, the charging time to initial hydrogen assisted cracking (t_B) is determined. From this, the charging time is gradually reduced until no cracking is observed.

Specimen No.	Bending stress σ (MPa)	Charging time t_B (min)	Hydrogen assisted crack length and duration of measurement					
			(h)	(mm)	(h)	(mm)	(h)	(mm)
4P-39	1100	35	0.0	0.0	70*	2.42	200	2.42
4P-40	1000	41	0.0	0.0	24	0.00	200	0.00
4P-41					24	0.00	200	0.00
4P-42	900	65	0.0	0.0	24	0.00	200	0.00
4P-43					24	0.00	200	0.00
4P-44	800	134	0.0	0.0	24	0.00	200	0.00
4P-45	700	430	0.0	0.0	24	0.00	200	0.00

* crack initiation determined by video recording

Table 5: Results for charging 4-point loaded specimens with hydrogen with no load and then with the application of mechanical load

Bend tests				
No.	Mechanical stress (MPa)	Charging time (min)	Diffusible hydrogen concentration (ppm)	Comments
9	1250	11.0 (100 % t_B)	0.67	Plastic range
10	1250	7.7 (70 % t_B)	0.49	
11	1250	5.5 (50 % t_B)	0.35	
12	1250	3.3 (30 % t_B)	0.36	
13a	0	11.0 (100 % t_B)	0.52	Deformed
13b	0	11.0 (100 % t_B)	0.39	Deformed
4-point bend tests				
No.	Mechanical stress (MPa)	Charging time (min)	Diffusible hydrogen concentration (ppm)	Comments
15	700	301 (70 % t_B)	0.9	Elastic range, not deformed
16	900	45.5 (70 % t_B)	0.58	Elastic range, not deformed
17	1100	24.5 (70 % t_B)	0.46	Plastic range
18a	0	35 (100 % t_B)	0.56	Not deformed, no mechanical load (t_B is load dependent)
18b	0	65 (100 % t_B)	0.87	
14	0	430 (100 % t_B)	1.31	

Table 6: Diffusible hydrogen concentration of bend test and 4-point bend test specimens

Specimen type	Charging time	Suitability of the test method for determining the sensitivity of materials	
		Component-like	Basic
4-point-bend test	Under mechanical load (Case 1)	0	+
	Before the application of mechanical load (Case 2)	0	+
Bend test	Under mechanical load (Case 1)	0	–
	Before the application of mechanical load (Case 2)	+	0

Table 7: Comparison of test methods with bend test and 4-point bend test

In the second step, two cases are observed during the charging time sequence. In Case 1, charging takes place under mechanical load. This corresponds to components which are subjected to charging by corrosion induced hydrogen penetration. In Case 2, the charging takes place before the mechanical load is applied and corresponds to components which are subjected to hydrogen penetration under production conditions. Both cases are suitable for investigating the comparative sensitivity of different materials. In this case, however, the time delay until the onset of hydrogen assisted damage must be taken into account.

On the specimens investigated, the cracks start out from the punched edge. The number of cracks was not taken into consideration. Outliers were occasionally observed. The suspected cause of this is also production related variations in the edge region. It is well known that residual stresses and associated residual strains have a considerable effect on the hydrogen related material properties.

On the bend specimens, an increase in hydrogen concentration was found which was almost proportional to the charging time. On 4-point loaded specimens, approx. ten times the charging time is required for a 400 MPa lower mechanical load to achieve twice the amount of diffusible hydrogen concentration which leads to cracking.

In our research, the duration of delay until first cracks appear ranges from a few hours to several days. During the four different investigations in this work, hydrogen assisted cracks appeared during a test period of 70 hours. Crack growth was only found in occasional cases after 70 hours. This is known for other types of specimens, such as the notched round tensile specimen according to ASTM F-519, and is taken into account with a scheduled test period of up to 200 hours [11]. A simple way to determine the exact times at which delayed cracks appear is to record the test setup by video instead of observing it at fixed times.

Bend tests. In order to determine the charging time t_B for the bend specimens, tests were carried out with different charging times for Case 1 and Case 2 to determine the time at which the start of cracking could be detected.

In Case 1, bend specimens were charged under mechanical load at 70 % t_B or 50 % and 30 % t_B, respectively.

With all specimens, it was found that delayed hydrogen assisted cracking occurred after charging regardless of the duration of charging. With a charging time of 70 % t_B, cracking led to complete fracture of the specimen within 24 hours during the period where it was not charged. With a charging time of 30 % t_B, cracks were found in all specimens within 24 hours and approx. one third of the specimens had fractured.

This means that the penetration of hydrogen leading to failure cannot be used to determine the sensitivity of materials to hydrogen if the test times are very short. Rather, the testing of delayed hydrogen assisted crack formation must be supported by a sufficiently long test period. No dependency on the delay of charging time (amount of hydrogen) can be derived from these figures.

In Case 2, bend specimens were charged at 100 % t_B in a unstressed state. Here, it was found that hydrogen assisted cracks or fractures occurred within 64 hours.

This confirms that delayed cracking must be taken into consideration with bend specimens in both cases.

At 0.39 and 0.53 ppm, the hydrogen uptake in the unstressed state is lower than it is in the strained state (0.67 ppm) for the same charging time.

4-point bend tests. In order to determine the charging time t_B for the 4-point loaded specimens, tests were carried out with different charging times for Case 1 and Case 2 to determine the time at which the start of cracking could be detected in relation to the mechanical stress.

In Case 1, 4-point loaded specimens were charged at 70 % t_B (t_B is load dependent) under mechanical stresses of 700, 800, 900, 1000 and 1100 MPa, respectively.

Delayed cracking occurred in the plastic range (1000 and 1100 MPa) during the test in six out of eight specimens and delayed cracking occurred in the elastic range (< 1000 MPa) after 24 hours in one out of eight specimens. Thus, the higher the load the sooner and more frequent the delayed cracking. A marked increase in susceptibility to hydrogen assisted damage was observed at a stress $\sigma \geq 1000$ MPa (transition to plastic range).

Delayed crack growth was observed with increasing test duration after charging in seven out of seventeen specimens. There were no fractures. This confirms that delayed cracking must be taken into consideration regardless of the test method.

In Case 2, 4-point loaded specimens were charged at 100 % t_B in an unstressed state. Here, it was found that no hydrogen assisted cracks or fractures occurred within 24 hours. After 70 hours, delayed cracking was found in one out of seven specimens.

This confirms that delayed cracking must be taken into consideration with 4-point loaded specimens in both cases.

At 0.46 to 0.9 ppm, the hydrogen uptake in the stressed state is lower (depending on load) than it is in the unstressed state (0.56 to 1.31 ppm) (depending on load) during longer charging times.

Conclusions

The results suggest that the specimen types investigated have a significant influence on the susceptibility to hydrogen assisted damage. Thus, the bend specimens which were previous distorted in the plastic range had a much higher sensitivity than the 4-point loaded specimens.

The bend specimens are suitable for determining the susceptibility of sheet metals to hydrogen assisted damage, taking into account the plastic deformation found in real components in a body structure. Even the smallest measured hydrogen concentration of 0.35 ppm leads to cracking, hydrogen exposure under load with plastic deformation being the most critical case.

The 4-point loaded specimens are suitable for determining susceptibility of sheet metals to hydrogen assisted damage in the elastic range under various mechanical stresses.

Test methods which only require a small amount of test equipment in particular, such as the 4-point loaded specimen test and the bend specimens test, have been shown to be suitable for determining the sensitivity of materials to hydrogen. When using these methods, the occurrence of delayed fractures or cracks must be taken into consideration. Susceptibility to hydrogen assisted damage in the plastic range is significantly higher. This is particularly important for the development of test methods designed to represent real sheet metal material applications, such as metal forming, notching and spot welding, where local stress peaks above the yield strength can occur.

It was also found that the amount of hydrogen which leads to delayed brittle fractures is less than the amount of hydrogen which leads to hydrogen assisted fractures during charging.

Charging via cathodic polarization under mechanical load until the specimen fractures, as shown in this work, is therefore only suitable to a limited extent for determining the sensitivity of materials to hydrogen assisted brittle fracturing. The amount of hydrogen supplied via cathodic polarization is high and the typical delay before hydrogen assisted crack formation has not been considered sufficiently.

Time-limited charging with or without mechanical load followed by removal under load is more suitable for meeting the requirements for the onset of delayed cracks or fractures in this case.

However, charging via cathodic polarization produces results with a very high level of reproducibility and the test parameters can be easily varied.

Outlook

Further investigations on continuous charging under mechanical stress with less amount of hydrogen could make it possible to develop test methods for differentiating between different materials. Additional methods to prevent low hydrogen concentrations from effusion like galvanic zinc coatings have to be tested for reliability. Furthermore, a modification of the bending test to apply different mechanical stresses as shown in the 4-point-bending test could be used as a very simple test method. The transferability of short-time test methods to in-service conditions and the life time of vehicles have to be investigated.

Acknowledgement

The authors wish to express their gratitude to Mr. Sturel of ArcelorMittal R&D, Maizières-lès-Metz, France, for carrying out the TDA measurements.

References

1 R. K. Pöpperling: Wasserstoff-induzierte Rissbildung an unlegierten und niedriglegierten Stählen (Hydrogen-induced cracking of carbon and low alloy steels), D. Kuron (Ed.): Wasserstoff und Korrosion, 2nd Ed., VIK, Bonn, Germany (2000), pp. 54-71
2 H. Pircher: Wasserstoff-induzierte Spannungsrisskorrosion an unlegierten und niedriglegierten Stählen (Hydrogen-induced stress corrosion cracking of carbon and low alloy steels), D. Kuron (Ed.): Wasserstoff und Korrosion, 2nd Ed., VIK, Bonn, Germany (2000), pp. 72-100
3 Q. Gao, F. Han, D. Wortberg, W. Bleck, M. Liewald: The impact of hydrogen on the formability of AHSS in Nakajima tests, AIP Publishing, ESAFORM 2016, Proceedings of the 19th International ESAFORM Conference on Material Forming, Nantes, France, 27-29 April 2016 DOI: 10.1063/1.4963626
4 M. Loidl: Development of a test method for characterizing advanced high strength car body steels regarding the susceptibility to hydrogen induced delayed cracking, Universität Stuttgart, Germany (2014), pp. 130-134 DOI:10.18419/opus-2286
5 R. J. H. Wanhill, S. A. Barter, S. P. Lynch, D. R. Gerrard: Prevention of hydrogen embrittlement in high strength steels, with emphasis on reconditioned aircraft components, NATO Science and Technology Organization: Corrosion Fatigue and Environmentally Assisted Cracking in Aging Military Vehicles: Research and Technology Organization (2011), pp. 20-1 - 20-52
6 D. Cornette, C. Allely, P. Dietsch, B. Weber, T. Sturel, C. Georges, S. G. Klose, J. Dold, T. Dettinger, D. Wortberg, T. Schweiker, P. Guillot, J. F. Beaudoin, R. Holbein, B. Kröger: No detrimental impact of car manufacturing process and simulation of vehicle in-service conditions on DP1180 hydrogen embrittlement, Proceedings of the Steely Hydrogen Conference 2014, Ghent, Belgium (2014), pp. aO4/46-56
7 ASTM G39-99 (2016): Standard Practice for Preparation and Use of Bent-Beam Stress-Corrosion Test Specimens, ASTM International, West Conshohocken, Pennsylvania, USA (1999)
8 H. Suzuki, K. Takai: Summary of round-robin tests for standardizing hydrogen analysis procedures, ISIJ International 52 (2012), No. 2, pp. 174-180 DOI:10.2355/isijinternational.52.174
9 C. Georges, B. Colinet, T. Sturel, D. Cornette, V. Lhoist: Development of electro galvanized AHSS with tensile strength of 1200 MPa for automotive application with no risk of delayed fracture, Proceedings of the Steely Hydrogen Conference 2014, Ghent, Belgium (2014), pp. pO4/536-541
10 S. Takagi, Y. Toji, M. Yoshino, K. Hasegawa: Hydrogen Embrittlement resistance evaluation of ultra high strength steel sheets, ISIJ International, Vol. 52 (2012), No. 2, pp. 316-322 DOI:10.2355/isijinternational.52.316
11 ASTM F519-13: Standard Test Method for Mechanical Hydrogen Embrittlement Evaluation of Plating/Coating Processes and Service Environments, ASTM International, West Conshohocken, Pennsylvania, USA (2013)

Abstract

Wasserstoffunterstützte Rissbildung in einem hochfesten Dualphasenstahl DP1180HY. Wichtige Ziele bei der Verwendung von hochfesten Stahlwerkstoffen in der Automobilindustrie sind die Gewichtsreduzierung und damit die Reduzierung des Energieverbrauchs von Kraftfahrzeugen. Geeignete Prüfmethoden müssen zur Charakterisierung der materialspezifischen Eigenschaften in Bezug auf Wasserstoff angewendet werden, so dass diese Materialien in Strukturbauteilen sicher eingesetzt werden können. Für diese Arbeit wurden Bügelproben und 4-Punkt-Biege-Proben verwendet. Beide Prüfmethoden haben spezifische Vor- und Nachteile und liefern aussagekräftige Ergebnisse hinsichtlich der zeitlichen Verzögerung bei wasserstoffgetriebenen Sprödbrüchen. Grundlegende Erkenntnisse wurden hinsichtlich des Prüfverfahrens und der Entwicklung von Prüfverfahren für die Auswirkungen von Wasserstoff auf Stahl bei der Herstellung und dem Betrieb der jeweiligen Bauteile gewonnen.

Bibliography

DOI 10.3139/120.111026
Materials Testing
59 (2017) 5, pages 430-437

ISSN 0025-5300

The authors of this contribution

Benjamin Kröger studied Mechanical Engineering with specialization in vehicle mechatronics at University of Applied Sciences Ravensburg-Weingarten, Germany and then received his Master's degree in Product Development in 2011. He has been part of the Steinbeis network since 2005 and was responsible for industrial and scientific projects until the end of 2014. In January 2015, the company Steinbeis Transfer Center for Corrosion and Corrosion Protection GmbH was transformed into a legally independent company and he took over the management together with Prof. Dr. R. Holbein. The areas of expertise in the fields of aerospace, automotive and other industries include the areas of materials, surface engineering, corrosion protection, electrochemistry, tribology and wear.

Prof. Dr.-Ing. Reinhold Holbein founded the Steinbeis Transfer Center for Corrosion and Corrosion Protection GmbH in Friedrichshafen, Germany in 1996, and since 2014 he has successfully continued this as a newly founded and legally independent company called "Steinbeis Transfer Center for Materials, Corrosion and Corrosion Protection. He worked in the company Dornier Luftfahrt GmbH in the area of materials, surface technology and corrosion protection. As a senior engineer for surface technology, he was responsible for aircrafts such as DO 228 and DO 328, among others. From 1994 to 2002, he taught at Albstadt University of Applied Sciences, Germany in the field of mechanical engineering, surface engineering, corrosion, tribology and aluminum alloys. In 2002, he moved to the University of Ravensburg-Weingarten, Germany and until 2015 he taught mechanical engineering, surface engineering and applied materials technology in the field of mechanical engineering.

Dr.-Ing. Stephan G. Klose graduated from the Technical University of Munich, Germany (Dipl.-Phys.) and received his Dr.-Ing. in Material Science from the Technical University Berlin, Germany in 1995. From 1996 to 2002, he held various positions at Audi AG in Ingolstadt, Germany in technical development, production and planning. In addition to materials and surface technology, plant engineering and production planning also played a decisive role. At the end of 2002, he took over different tasks at Daimler AG in the development of passenger cars with regard to corrosion protection, materials and surface technology. Currently, he is a senior manager at Daimler AG in Sindelfingen, Germany, responsible among others, for advanced materials and technologies in pre-development, focusing on lightweight construction with ultra-high strength steels, aluminum and magnesium materials for car body applications in passenger cars and commercial vehicles.